Neutron-Diffraction Study of Quadrupolar Order in TmTe: First Evidence for a Field-Induced Magnetic Superstructure

P. Link,[1] A. Gukasov,[1] J.-M. Mignot,[1] T. Matsumura,[2] and T. Suzuki[2]
[1]*Laboratoire Léon Brillouin, CEA-CNRS, CEA-Saclay, 91191 Gif sur Yvette, France*
[2]*Department of Physics, Tohoku University, Sendai 980-77, Japan*
(Received 4 February 1998)

The intriguing phase transition discovered recently in TmTe at $T_Q = 1.8$ K is characterized as antiferroquadrupolar by neutron diffraction. In an applied magnetic field, the underlying ordered structure of the Tm quadrupole moments is disclosed by the appearance of an antiferromagnetic component of the magnetic dipole moments. This induced structure is described by the wave vector $\boldsymbol{k} = (1/2, 1/2, 1/2)$ for both field directions $\boldsymbol{H} \parallel (111)$ and $\boldsymbol{H} \parallel (001)$, but the staggered component μ_{AF}, oriented along a twofold cubic axis normal to the field, is much stronger (about $1.5\mu_B$) in the former case. [S0031-9007(98)06060-8]

PACS numbers: 75.25.+z, 61.12.Ld, 63.20.Kr, 75.30.Kz

There is currently an upsurge of interest for magnetic phenomena in localized electron systems involving an interplay between spin and orbital degrees of freedom, as well as a coupling to the lattice. Such situations are exemplified by the orbital order in manganese perovskites and other related transition-metal compounds [1], by the Jahn-Teller effect in rare-earth insulators such as zircons or spinels [2], as well as by quadrupolar interactions in a small class of intermetallic f-electron compounds (TmZn, $TmGa_3$, CeB_6, etc.) [3]. One important common feature of these systems is the possible occurrence of a phase transition below which the electric quadrupole moments associated with the $3d$ or $4f$ electron wave functions become long-range ordered. In the case of rare-earth compounds, to which we will restrict our discussion in the following, it is important to distinguish between insulating materials, in which the interactions between quadrupoles take place primarily via a virtual exchange of phonons, and intermetallic systems, where an indirect RKKY-like, interaction, mediated by conduction electrons, prevails [4]. Because quadrupolar moments are described by second-rank tensor operators, the physics of their ordered states is obviously much more intricate than for magnetic dipole moments. The different types of order found in real materials can be broadly categorized as ferroquadrupolar (FQ) if the value of the order parameter is uniform from site to site, and antiferroquadrupolar (AFQ) whenever the structure presents a staggered character [5]. The first class contains essentially all insulating materials reported to date, and a majority of the intermetallic systems. On the other hand, our experimental knowledge of AFQ order is based on a very limited number of examples. Among them, CeB_6 is of special significance because it is the only case where the AFQ character could be proved unambiguously by neutron diffraction experiments [6]. However, this compound is not particularly simple, because its low-temperature properties are strongly affected by the Kondo effect of cerium and, from the point of view of neutron experiments, because the magnetic moment of Ce is small and the absorption cross section of boron rather large, even in isotopic samples. Therefore, the recent discovery of a new phase transition, suggestive of AFQ order, in TmTe [7] has attracted considerable attention. Until then, this material (NaCl structure, space group $Fm\bar{3}m$, $a = 6.357$ Å) was considered a rather ordinary magnetic semiconductor with a divalent TM^{++} state ($4f^{13}$, $^2F_{7/2}$ configuration) and a low Néel temperature of about 0.4 K [8]. It thus came as a surprise that specific heat, elastic constant, and thermal expansion measurements on high-quality single crystals [7,9,10] consistently show an anomaly at about $T_Q = 1.8$ K, clearly distinct from the specific heat peak at $T_N = 0.4$ K. The magnetic phase diagram is reminiscent of CeB_6, with a pronounced increase of T_Q in an applied field for all directions of H, followed by a decrease in higher fields for $\boldsymbol{H} \parallel (001)$ only. From the peculiar shape of this phase diagram and the T variations of the elastic constants, it was suggested in Ref. [7] that the new phase below T_Q corresponds to an ordered state of the Tm quadrupole moments. To confirm this assumption, a strong piece of evidence would come from the direct observation of a staggered structure by neutron diffraction. However, since neutrons have no significant coupling to quadrupole moments, such a measurement requires the application of a magnetic field so that, as was found in CeB_6, the underlying AFQ order may be reflected into the structure of magnetic dipole moments.

In this Letter, we report the first experimental evidence that such a field-induced antiferromagnetic structure indeed exists in TmTe, strongly supporting the assumption of an AFQ order in this material. Furthermore, we show that relevant information regarding the nature of the quadrupolar order parameter can be obtained from a thorough symmetry analysis of the magnetic diffraction results.

The measurements were carried out on the two-axes lifting-counter diffractometers 6T2 and 5C1 at the reactor Orphée in Saclay using neutron wavelengths of 0.090 and 0.084 nm, respectively, with a primary beam collimation of 50′. Second-order contamination was

suppressed to less than 0.01% by means of an erbium filter. Single-crystalline TmTe was prepared by induction melting of high-purity constituents inside a vacuum-sealed tungsten crucible [9]. Two different specimens, of dimensions $4 \times 5 \times 3$ mm^3 and $4 \times 3 \times 9$ mm^3, were used, respectively, for the measurements with $\boldsymbol{H} \parallel (001)$ and $\boldsymbol{H} \parallel (111)$. In the latter case, however, a small misalignment was found to exist, essentially caused by a rotation of the crystal by about 10° around the $(1\,-1\,0)$ axis. Experiments were carried out in the temperature range between $T_{\min} = 1.7$ K and $T_{\max} = 10$ K. Vertical magnetic fields H of up to 12 T (6T2) and 7.5 T (5C1) were generated using commercial cryomagnet systems. The magnetic structure refinements were performed using the programs MAGLSQ and MLSTWN from the Cambridge Crystallography Subroutine Library [11].

For normalization purposes, the integrated intensities (obtained by ω scans) of a large number of nuclear reflections, with scattering angles up to $\sin\theta/\lambda = 7$ nm^{-1}, were measured for both samples in the paramagnetic phase ($T = T_{\max}, H = 0$). Since all atomic positions are fixed in the NaCl-type structure, the measured intensities were used to refine the overall scale factor and one correction factor Ω_{fac} accounting for the intensity loss at large diffraction angles occurring in ω scans in comparison with $(\omega, 2\theta)$ scans. Both parameters were kept fixed in all subsequent refinements of magnetic reflections measured under the same conditions. Extinction corrections were not found to improve the quality of the fits and were therefore neglected in the following data treatment.

Cooling the sample in zero field to $T = T_{\min}$, i.e., below the transition temperature T_Q reported in Ref. [7], did not generate any additional superstructure reflections, in agreement with the previous results of Lassailly *et al.* [8] who found magnetic order only below $T_N = 0.4$ K. On the other hand, the application of a magnetic field at $T = T_{\min}$ resulted not only in the normal increase of intensity at the nuclear peak positions reflecting the uniform induced (ferro)magnetic component, but also in the appearance of a new set of superstructure reflections. For both field directions, the induced structure corresponded to the wave vector $\boldsymbol{k} = (1/2, 1/2, 1/2)$. Experimentally, reflections associated with all four components $\boldsymbol{k}_1 = (1/2, 1/2, 1/2)$, $\boldsymbol{k}_2 = (1/2, 1/2, -1/2)$, $\boldsymbol{k}_3 = (1/2, -1/2, 1/2)$, and $\boldsymbol{k}_4 = (-1/2, 1/2, 1/2)$ of the star of $\{\boldsymbol{k}\}$ were clearly observed. As an example, the field dependence of the $(3/2, -1/2, -1/2)$ reflection, associated with the vector $\boldsymbol{k}_1$, is displayed in Fig. 1. Scans performed systematically along high-symmetry directions revealed no further peaks at other reciprocal-lattice points.

With increasing temperature, all superstructure peaks disappeared for $T > T_Q$. The intensities of the strongest reflections, $(3/2, 1/2, 1/2)$ for $\boldsymbol{H} \parallel (001)$ and $(3/2, -1/2, -1/2)$ for $\boldsymbol{H} \parallel (111)$, were monitored as a function of temperature and applied magnetic field, leading to a (T, H) phase diagram in good agreement with the specific-heat results of Ref. [7], as shown in the inset of Fig. 1 [12]. In particular, T_Q initially increases with H for both field directions, then, above $H \sim 5$ T, it becomes nearly constant for $\boldsymbol{H} \parallel (111)$, whereas it decreases drastically for $\boldsymbol{H} \parallel (001)$.

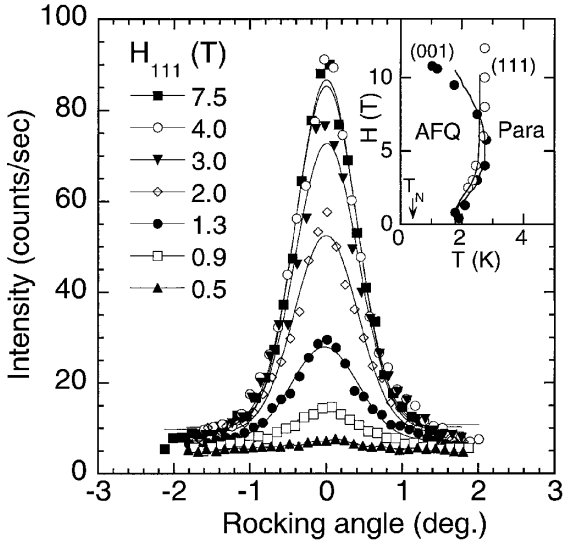

FIG. 1. Induced AF Bragg peak $(3/2, -1/2, -1/2)$ for different magnetic fields $0.5 \leq H_{111} \leq 7.5$ T applied along (111) at $T = 1.7$ K; inset: magnetic phase diagram of TmTe; open and closed symbols: neutron results for $\boldsymbol{H} \parallel (111)$ and $\boldsymbol{H} \parallel (001)$, respectively; solid lines: corresponding phase boundaries derived from specific-heat measurements (reproduced from Ref. [9]).

The magnetic origin of the superstructure reflections observed below T_Q can be deduced from the considerable decrease of their intensities at large momentum transfers, approximately following the variation of the magnetic form factor of Tm^{2+} [13]. Indeed, this behavior is just the opposite of what is expected in the case of a structural distortion. Furthermore, especially in the case of $\boldsymbol{H} \parallel (111)$, the peak intensities are quite strong, and the atomic displacements required to account for such values would be unphysical. Therefore, the results indicate that the uniform applied field actually induces an antiferromagnetic component of the Tm moments characterized by the wave vector $\boldsymbol{k} = (1/2, 1/2, 1/2)$.

Since we are interested in a possible order of quadrupole moments in TmTe, which would result in singling out one particular direction in each Tm site, it is important not just to know the magnetic wave vector, but also to work out a complete solution of the structure, including the direction and magnitude of the Fourier components of the moment. This requires the collection of an extensive set of data at the lowest temperature for reflections associated with each wave vector $\boldsymbol{k}_1$ to $\boldsymbol{k}_4$. For $\boldsymbol{H} \parallel (111)$, measurements were performed in applied fields $H = 2, 4, 6$, and 7.5 T on 6T2 and $H = 5$ T on 5C1. Even at relatively low fields ($H = 2$ T), the intensities of the $\boldsymbol{k}_1$ reflections are considerably larger than those associated with the other three members of the star of $\{\boldsymbol{k}\}$. As H increases, the former peaks are strongly enhanced, whereas the latter

become even weaker, so that the intensity ratio reaches about 1 order of magnitude for $H = 5$ T. This behavior suggests a single-$\boldsymbol{k}$ antiferromagnetic structure, in which each $\boldsymbol{k}$ vector is associated with one $\boldsymbol{k}$ domain, and should thus be treated individually.

Out of 140 superstructure reflections collected at $T = T_{\min}$ in a field of $H = 5$ T, 59 belonged to the strong $\boldsymbol{k}_1$ domain. Let us concentrate on these data by first considering the simplest cases (the subscript of $\boldsymbol{k}$ will be omitted in the rest of this section). The solution $\boldsymbol{m_k} \parallel \boldsymbol{k}$ can be readily discarded because reflections having $\boldsymbol{Q} \parallel \boldsymbol{k}$ have been found to exist. For $\boldsymbol{m_k} \perp \boldsymbol{k}$, one needs to consider the existence of so-called "S domains," corresponding to magnetic components μ_{AF} oriented along different, symmetrically equivalent directions, e.g., $(1\,-1\,0)$, $(1\,0\,-1)$, and $(0\,1\,-1)$. In the plane perpendicular to $\boldsymbol{k}$, two sets of high-symmetry directions exist, namely, $(1\,-1\,0)$ and $(1\,1\,-2)$. In the inset of Fig. 2, we have plotted the angular factor I_{norm}, defined as the squared ratio of the (measured) magnetic structure factor divided by the corresponding (calculated) Tm^{2+} form factor [13], as a function of the angle α between the scattering vector $\boldsymbol{Q}$ and the $(1\,-1\,0)$ direction. A maximum is clearly seen at $\alpha = 90°$, suggesting that one main S domain, with a Fourier component $\boldsymbol{m_{ks}}$ directed along $(1\,-1\,0)$, exists and prevails over the other two symmetry-equivalent domains corresponding to $(1\,0\,-1)$ and $(0\,-1\,1)$. In the figure, the solid line representing the calculated dependence of the angular factor for this domain alone is seen to reproduce quite well the general shape of the experimental data points. The agreement can still be improved (especially regarding the finite intensities measured near $\alpha = 0°$ and 180°), by allowing for a minor population of the other two S domains. The results of numerical refinements of the measured squared structure factors support the above analysis, as the best reliability factor ($R = 0.12$) was obtained by assuming the three S domains to have identical moments, normal to the $\boldsymbol{k}$ vector and oriented along the $\langle 1\,-1\,0\rangle$ directions, but allowing their relative populations to vary. The magnitude of the Fourier component obtained from the refinement is $\mu_{\mathrm{AF}} = 1.5\mu_B$ at $T = 1.7$ K. The population ratios (65:12:23) confirm that one S domain strongly dominates. The orientation matrix actually indicates that the $\langle 1\,-1\,0\rangle$ axis for this domain was oriented almost perfectly perpendicular to the field direction, whereas, for the other domains, its angle with respect to H was only about 80°. A similar treatment can be applied to the other $\boldsymbol{k}$ domains, but the analysis is less reliable because the experimental intensities are much weaker. The data could be satisfactorily refined with the assumption that the Fourier components $\boldsymbol{m_k}$ are again oriented along the twofold axes which are perpendicular to both $\boldsymbol{H}$ and $\boldsymbol{k}$ (leaving only one S domain possible in this case), but alternative solutions cannot be ruled out.

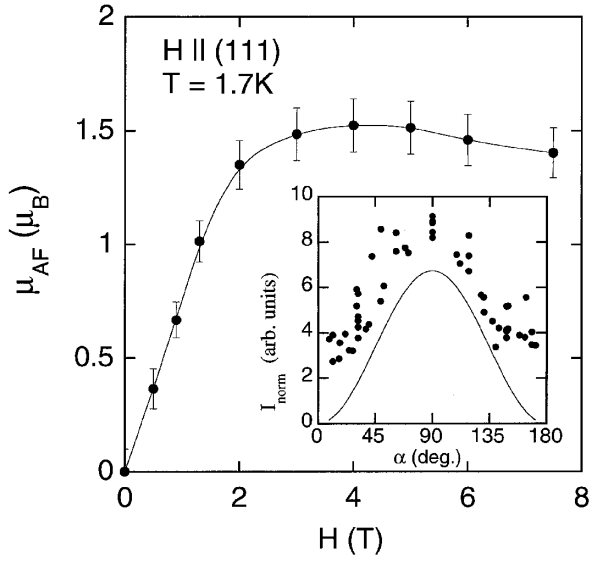

FIG. 2. Field dependence of the component μ_{AF}; inset: angular dependence of the normalized intensities of the AF reflections (see text); •, experimental data; solid line: calculated angular dependence for a single domain with $\boldsymbol{m_{ks}} \parallel (1\,-1\,0)$.

Knowing the changes in $\boldsymbol{k}$-domain populations, we can now derive the variation of the staggered component μ_{AF} in an applied field $\boldsymbol{H} \parallel (111)$ from the measured integrated intensities of the AF peak displayed in Fig. 1. The resulting curve, normalized to the above value of $1.5\mu_B$ at $H = 5$ T, is plotted in Fig. 2. It exhibits a clear saturation at about 4 T, followed by a plateau, or a slow decrease, in higher fields.

The value of the field-induced uniform magnetic component can be derived from the magnetic intensities superimposed on the nuclear peaks, using the Tm^{2+} form factor calculated according to Ref. [13]. The refinement gives a moment of $2.6\mu_B$ for $H = 5$ T. This value, as well as the field dependence obtained from the neutron data, agrees well with bulk magnetization measurements [9]. From the above results, the magnetic structure at $T_{\min}$ in an applied field of 5 T can be described as a stacking of ferromagnetic planes perpendicular to the (111) direction (same as the field direction in the case of the $\boldsymbol{k}_1$ domain), with moments of $\approx 3\mu_B$ tilted alternatively by about $\pm 30°$ out of normal to the plane toward the $(1\,-1\,0)$ axis.

For the other field direction studied, $\boldsymbol{H} \parallel (001)$, the reflections associated with all wave vectors, from $\boldsymbol{k}_1$ to $\boldsymbol{k}_4$, which are now symmetry equivalent, were found to have comparable intensities. On the other hand, this situation makes it impossible to distinguish between single-k and the multi-k structures. Quantitative refinements were hindered by the weakness of the magnetic signal and the insufficient number of measured reflections. A rough estimate based on the data at $T = T_{\min}$ and $H = 4$ T gives an antiferromagnetic moment of $\mu_{\mathrm{AF}} \approx 0.4\mu_B$ and a uniform component of about $2.2\mu_B$.

At first sight, inducing an AF moment component on the TM sublattice by the application of a uniform external field may look surprising. This, however, merely reflects the fact that the response of the Tm magnetic moments to the applied field is constrained by the quadrupole order

built up below T_Q. The present results thus confirm the suggestion of Refs. [7,9], that the phase transition at T_Q occurring in zero field is of AFQ type, with a characteristic wave vector $\boldsymbol{k} = (1/2, 1/2, 1/2)$. In this respect, a strong analogy exists between the present compound and CeB_6. In a recent series of papers, Shiina and co-workers [14,15] have classified possible ordered phases in CeB_6 (cubic crystal field with a well-isolated Γ_8 quartet ground state) in terms of their symmetry properties, and established relations between the quadrupole order parameters and the field-induced dipole moments. In TmTe, the local symmetry of the Tm site is also cubic, and recent neutron scattering results [16] have been ascribed to a crystal-field level scheme in which the ground state is again Γ_8, but the overall splitting does not exceed 15 K, as compared to 540 K in CeB_6. If we confine ourselves to the lowest states within the quartet, the analysis of Ref. [14] is readily applicable to TmTe. In particular, for the field directed along the (111) axis, three different types of AFQ order can be distinguished according to the direction of the induced staggered component of the magnetic dipole moments. In our case, the measurements performed at $H_{111} = 5$ T indicated that the induced component μ_{AF} is parallel to $(1\,-1\,0)$ (angular-momentum operator $J_x - J_y$). This is compatible with quadrupolar order parameters of types O_2^2 and $O_{yz} - O_{zx}$. In principle, similar arguments can be given for other field orientations but, as already mentioned, the direction of the induced AF component could not be determined in our measurements with $\boldsymbol{H} \parallel (001)$. However, if one follows the arguments of Ref. [15] and assumes that the field can be rotated from (111) to (001) inside the $[1\,-1\,0]$ plane without the system undergoing a phase transition, the (odd) parity of the quadrupole order parameter with respect to a mirror reflection across the plane must be preserved. Among the solutions listed in Ref. [14], this condition leaves only two possibilities, namely, O_2^2 and $O_{yz} - O_{zx}$ (linear combination of the degenerate solutions O_{yz} and O_{zx}). The important point is that, in the former case, the field-induced AF component of the magnetic moment is predicted to vanish, whereas it should exist in the latter case. Thus experimentally, the much weaker AF moment measured for $\boldsymbol{H} \parallel (001)$, as compared to $\boldsymbol{H} \parallel (111)$, seems to favor the O_2^2 solution. A more realistic model, taking into account the symmetry lowering in the ordered phase of TmTe, should clarify this point. It is important to realize that, even though we have been using the analogy between CeB_6 and TmTe as a guideline in the preceding discussion, the microscopic mechanisms responsible for the quadrupole order in these compounds could be quite different. In TmTe, the role of conduction electrons at low temperature is most likely negligible and the coupling is thus expected to take place primarily through the channel of phonons. In CeB_6, on the other hand, despite significant theoretical progress in the understanding of the phase diagram [14,17,18], the microscopic origin of the so-called "phase II" is not yet fully clarified. In TmTe, more precise experiments are needed to search for weak structural distortions and the possibility of anomalies in the lattice dynamics at low temperature should be checked in relation with the appearance of the AFQ phase. The role of quadrupolar interactions in the AF order setting in below $T_N \sim 0.4$ K is another important question, especially since both phases appear to be characterized by the same wave vector $\boldsymbol{k} = (1/2, 1/2, 1/2)$. Neutron experiments below 1 K are needed to clarify this point.

The authors thank P. Fouilloux for his help during the experiments. They are grateful to P. Haen, T. Kasuya, P. Morin, F. Onufrieva, D. Schmitt, and R. Shiina for useful comments about their previous results, and stimulating discussions. This work has been supported by the Commission of the European Union through TMR Grant No. ERB 400 1 GT 95 5456.

[1] K. I. Kugel and D. I. Komskii, Sov. Phys. Usp. **25**, 231 (1982); D. I. Khomski and G. A. Savatzky, Solid State Commun. **102**, 87 (1997).
[2] G. A. Gehring and K. A. Gehring, Rep. Prog. Phys. **38**, 1 (1975).
[3] P. Morin and D. Schmitt, in *Ferromagnetic Materials*, edited by K. H. J. Buschow and E. P. Wohlfarth (Elsevier, Amsterdam, 1990) Vol. 5, p. 1.
[4] P. M. Levy, P. Morin, and D. Schmitt, Phys. Rev. Lett. **42**, 1417 (1979).
[5] More correctly, the terms "ferriquadrupolar" and "multiaxial" have been introduced in Ref. [3] to denote two distinct types of nonuniform ordered quadrupole structures which could in principle exist in real systems.
[6] J. M. Effantin *et al.,* J. Magn. Magn. Mater. **47&48**, 145 (1985).
[7] T. Matsumura *et al.,* Physica (Amsterdam) **223B&224B**, 385 (1996).
[8] Y. Lassailly *et al.,* Solid State Commun. **52**, 717 (1984).
[9] T. Matsumura *et al.,* Physica (Amsterdam) **206B&207B**, 380 (1995).
[10] P. Haen (private communication).
[11] P. J. Brown and J. C. Mattewman, "The Cambridge Crystallography Subroutine Library-Mark 4 Users' Manual," Rutherford Appleton Laboratory Internal Report No. RAL-93-009, 1987 (unpublished).
[12] Because of temperature gradients existing in the cryomagnet system, all experimental T values plotted in the inset of Fig. 1 had to be corrected by a fixed amount in order to achieve consistency between the specific-heat and neutron data.
[13] J. X. Boucherle, D. Givord, and J. Schweizer, J. Phys. (Paris) Colloq. **43**, C7-199 (1982).
[14] R. Shiina, H. Shiba, and P. Thalmeier, J. Phys. Soc. Jpn. **66**, 1741 (1997).
[15] R. Shiina *et al.,* (to be published).
[16] E. Clementyev *et al.,* Physica (Amsterdam) **230B–232B**, 735 (1997).
[17] G. Uimin, Y. Kuramoto, and N. Fukushima, Solid State Commun. **97**, 595 (1996).
[18] T. Kasuya, J. Phys. Soc. Jpn. (to be published).